

He-McKellar-Wilkens topological phase in atom interferometry

S. Lepoutre, A. Gauguet, G. Tréneç, M. Büchner, and J. Vigué

Laboratoire Collisions Agrégats Réactivité-IRSAMC
Université de Toulouse-UPS and CNRS UMR 5589, Toulouse, France
e-mail: jacques.vigue@irsamc.ups-tlse.fr
(Dated: November 4, 2018)

We report the first experimental test of the topological phase predicted by He and McKellar and by Wilkens in 1993: this phase, which appears when an electric dipole propagates in a magnetic field, is connected to the Aharonov-Casher effect by electric-magnetic duality. The He-McKellar-Wilkens phase is quite small, at most 27 mrad in our experiment, and this experiment requires the high phase sensitivity of our atom interferometer with spatially separated arms as well as symmetry reversals such as the direction of the electric and magnetic fields. The measured value of the He-McKellar-Wilkens phase differs by 31% from its theoretical value, a difference possibly due to some as yet uncontrolled systematic errors.

PACS numbers: 03.65.Vf; 03.75.Dg; 39.20.+q

In quantum mechanics, propagation can be modified without any force, the first example being the Aharonov-Bohm effect [1] discovered in 1959: a magnetic field shifts the fringes of an electron interferometer, even if the field vanishes on the electron paths. This was the discovery of topological phases [2], which differ considerably from ordinary dynamic phases because they are independent of the particle velocity and non-reciprocal, i.e. they change sign when propagation is reversed. In 1984, Aharonov and Casher [3] discovered another topological phase, which appears in a matter wave interferometer operated with a particle carrying a magnetic dipole, the interferometer arms encircling a line of electric charges. In 1993, He and McKellar [4] applied electric-magnetic duality [5] to the Aharonov-Casher phase, thus exhibiting a topological phase when the particle carries an electric dipole and the interferometer arms encircle a line of magnetic monopoles: this phase appeared as speculative but a possible experiment was rapidly proposed by Wilkens [6]. Whereas the Aharonov-Bohm and Aharonov-Casher (AC) effects were rapidly tested by experiments [7–12], no experimental test of the He-McKellar-Wilkens (HMW) phase has been available so far. Here, we report the first experimental attempt to detect the HMW phase, with results in reasonable agreement with theory. The HMW phase is the last member of the family of topological phases when free particles propagate in electromagnetic fields [13, 14]: one might expect similar phases for higher order electromagnetic multipoles but the calculated values for quadrupoles [15] are so small that their detection is presently out of reach.

Although Wilkens experiment proposal [6] is 18 years old, no experimental proof of the HMW phase has been reported. A test was discussed in 1996 by Wei *et al.* [16] and by Schmiedmayer *et al.* [17] and an experiment with a superfluid helium interferometer was proposed in 2009 by Sato and Packard [18], without any published result yet. Let us compare the detection of the AC and HMW phases, in order to understand why this test is

difficult. All accurate tests of the AC phase [10–12] have used a Ramsey interferometer [19], in which the particle propagates in a superposition of two spin states: this type of interferometer is ideal for the detection of a spin-dependent phase and it provides an excellent cancellation of systematic errors. The use of a Ramsey interferometer for the HMW phase would require the production of a quantum superposition of states with opposite electric dipole moments, which is feasible if states of opposite parity are quasi-degenerate [14], a situation which does not exist with ground state atoms. Consequently, the HMW phase must be measured by alternating field configurations and by studying differences of measured phases: this procedure makes an experiment more subject to systematic errors than Ramsey interferometry. In addition, in order to create a non-zero HMW phase shift, the two interferometer arms must propagate in different electric or magnetic fields, which is possible only if the two arms are spatially separated. Following the pioneering work of Pritchard and co-workers [17, 20], very few separated-arm atom interferometers have been built.

Although not associated with a classical force, the AC and the HMW phases can be explained by the interaction of a dipole with a motional field [14]. The HMW phase is due to the interaction of an electric dipole \mathbf{d} with the motional electric field $\mathbf{E}_{mot} = \gamma \mathbf{v} \times \mathbf{B}$ where \mathbf{v} is the atom velocity, \mathbf{B} is the magnetic field and $\gamma = 1/\sqrt{1 - v^2/c^2} \simeq 1$ is the relativistic factor. $U = -\mathbf{d} \cdot \mathbf{E}_{mot}$ is the interaction energy, which induces the HMW phase shift:

$$\varphi_{HMW} = \oint U dt / \hbar \quad (1)$$

where the closed loop follows the interferometer paths. Because of parity, atoms or molecules do not have a permanent dipole and an electric field \mathbf{E} is needed to induce a dipole $\mathbf{d} = 4\pi\epsilon_0\alpha\mathbf{E}$, where α is the electric polarizability. Finally, the HMW phase shift is given by:

$$\varphi_{HMW} = \oint (\mathbf{d} \times \mathbf{B}) \cdot \mathbf{v} dt / \hbar \quad (2)$$

Because $\mathbf{v} dt$ is the infinitesimal path length, φ_{HMW} is independent of the modulus v of the atom velocity but it changes sign with the direction of propagation, and it is maximum when \mathbf{E} , \mathbf{B} and \mathbf{v} are orthogonal.

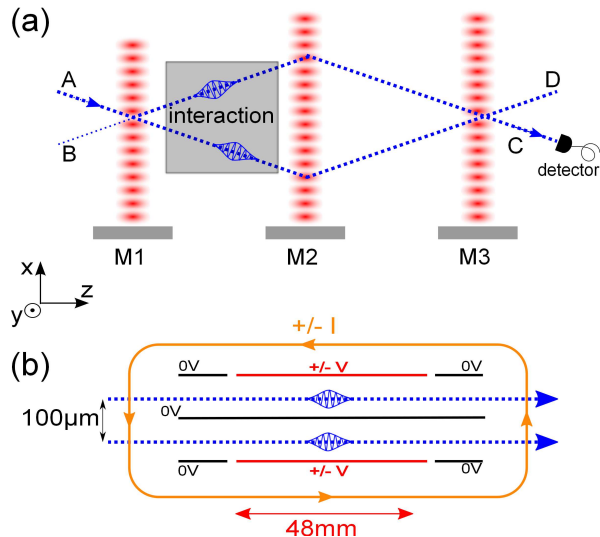


FIG. 1: (Color online) Schematic top views of the setup. Panel a: our atom interferometer, with two entrances A and B and two exits C and D (C is detected). An atomic beam (dotted blue lines) entering by A is diffracted by three quasi-resonant laser standing waves produced by the mirrors M_i . The interaction region is placed where the distance between interferometer arms is largest, close to $100 \mu\text{m}$. Panel b: the interaction region producing the electric and magnetic fields (not to scale). The interferometer arms (dotted blue lines) are separated by a septum, which is the common electrode of two plane capacitors producing opposite electric fields (high voltage electrodes in red; grounded electrodes in black). Two rectangular coils (brown rectangle) produce the magnetic field.

To detect the HMW phase, we use a Mach-Zehnder atom interferometer [21] shown in fig. 1a. A supersonic lithium beam (mean velocity near 1000 m/s with a distribution half-width close to 100 m/s) is strongly collimated and then diffracted by three laser standing waves in the Bragg regime: the laser frequency is chosen such that only the dominant lithium isotope ${}^7\text{Li}$ contributes to the signal [21, 22]. The diffraction events play the roles of beam-splitters and mirrors for the atomic wave. This interferometer produces two output beams, labeled C and D on fig. 1a, with complementary fringe signals. Beam C is selected by a slit and the atoms of this beam are ionized by a Langmuir-Taylor "hot-wire" detector [23]. The resulting ions are counted, thus providing the interferometer signal I given by:

$$I = I_0 [1 + \mathcal{V} \cos(\varphi_p + \varphi_d)] \quad (3)$$

I_0 is the mean intensity and \mathcal{V} is the fringe visibility. The phase φ_p is due to perturbations. The phase φ_d , due to atom diffraction, depends on the positions of the laser standing wave mirrors M_i . To record interference fringes (see fig. 2), we move mirror M_3 with a piezoelectric device and its displacement, measured by a Michelson interferometer, gives very accurately the variations of φ_d . Typical values of the mean intensity and of the fringe visibility are $I_0 \approx 50000 \text{ atoms/s}$ and $\mathcal{V} \approx 70\%$, leading to a phase sensitivity near $20 - 30 \text{ mrad}/\sqrt{\text{Hz}}$.

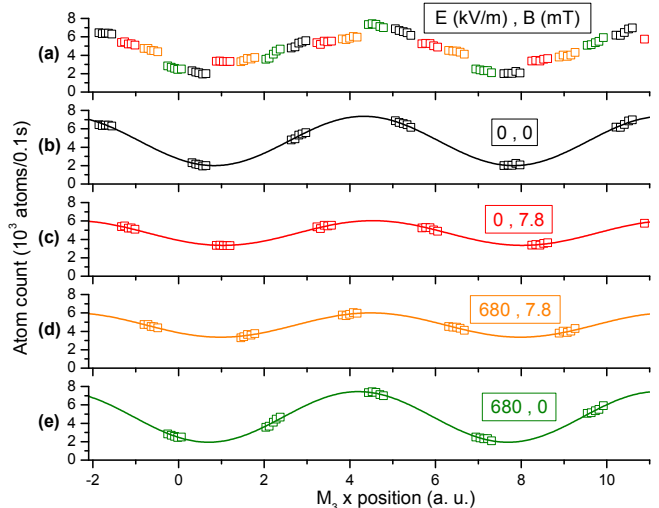


FIG. 2: (Color online) Panel a: the atom interferometer signal is plotted as a function of M_3 x -position, using the 4-field configuration procedure with $E = 680 \text{ kV/m}$ and $B = 7.8 \text{ mT}$. In panels b-e, the signals corresponding to each field configuration, are plotted with their best fits. The mean detected flux $I_0 \approx 47 \times 10^3 \text{ atoms/s}$ is constant. We use the no-field case as reference for visibility ($\mathcal{V}_0 = (57.2 \pm 0.6)\%$) and phase. In panel c, $\mathcal{V}(0, I)/\mathcal{V}_0 = (50.0 \pm 1.2)\%$ and $\varphi_B(I) = -183 \pm 25 \text{ mrad}$. In panel d, $\mathcal{V}(V, I)/\mathcal{V}_0 = (48.7 \pm 0.2)\%$ and $\varphi_{E+B}(V, I) = -139 \pm 24 \text{ mrad}$. In panel e, $\mathcal{V}(V, 0)/\mathcal{V}_0 = (102.4 \pm 1.6)\%$ and $\varphi_E(V) = 118 \pm 18 \text{ mrad}$. From these measurements, we get $\varphi_{EB}(V, I) = (-74 \pm 35) \text{ mrad}$. The average over about 100 similar scans produce phase measurements with a few mrad error bar.

The interaction region is schematically represented in fig. 1b (more details in [5]): homogeneous electric fields are produced by two plane capacitors sharing a thin "septum" electrode [24], which is inserted between the two interferometer arms without modifying their propagation. With a 1.10 mm electrode spacing, the electric field is $E(\text{kV/m}) \approx 0.9V$ where the applied voltage V (Volt) can be positive or negative, in order to test field reversal. The double capacitor is placed inside a pair of coils producing a fairly homogeneous magnetic field: the use of coils rather than permanent magnets limits the field value near 14 mT but gives rise to a much better control and permits field reversal. For a current I circulating in the coils, the field B at the center is given by $B/I \approx 0.56 \text{ mT/A}$.

This configuration with opposite electric fields on the two arms, proposed by Wei et al. [16], differs from the idea of He, McKellar and Wilkens [4, 6] in which the same electric dipole propagates in opposite magnetic fields but we think that the phase shift predicted by equation 2 is truly a HMW phase shift [5]. We have replaced the charged wire of Wei et al. [16] by plane capacitors to improve the field homogeneity and to minimize the dispersion of the polarizability phase (a large dispersion reduces the fringe visibility). With this interaction region and lithium atoms [25], the HMW phase shift predicted by equation (2) is $\varphi_{HMW}(V, I)(\text{rad}) = -1.28 \times 10^{-6}VI$, corresponding to a maximum value $|\varphi_{HMW}|_{max} = 27$ mrad for $|V| = 800$ V and $|I| = 25$ A.

Let $\varphi_{E+B}(V, I)$ be the measured phase shift when the electric and magnetic fields are both applied. φ_{E+B} includes the HMW phase shift but also the dynamic phase shifts [26] induced by each field acting separately. The electric field induces a Stark (or polarizability) phase shift [24] $\varphi_S = -2\pi\varepsilon_0\alpha \oint \mathbf{E}^2 dt/\hbar$. We tune the ratio of the voltages applied to the capacitors to ensure $\varphi_S \lesssim 100$ mrad, a very small value compared to the phase shifts induced on each arm which can exceed 300 rad.

The magnetic field induces a Zeeman energy shift $U_Z(F, m_F)$, function of the F, m_F hyperfine sub-level, and a phase shift [22, 27] given by $\varphi_Z(F, m_F) = \oint U_Z(F, m_F, B) dt/\hbar$. If a magnetic field $B = 14$ mT was applied to one arm only, the Zeeman phase shift would be extremely large, $\varphi_Z(F = 2, m_F = \pm 2) \approx \pm 10^5$ rad. This phase shift would be perfectly canceled if the magnetic field had exactly the same value on the two arms but a weak field gradient exists near the septum, sufficient to induce a Zeeman phase shift $\varphi_Z(F = 2, m_F = \pm 2) \approx \pm 11$ rad when $B = 14$ mT. The detected signal is an average over the ground state sub-levels with almost equal contributions [5, 22]. These sub-levels form 4 pairs with opposite Zeeman phase shifts, so that the measured Zeeman phase shift φ_B is very weak but the large dispersion of φ_Z with F, m_F reduces the fringe visibility. To reduce the Zeeman phase shifts, another coil producing an opposite magnetic field gradient was introduced outside the interaction region of fig. 1b, and this compensation is excellent when hyperfine uncoupling is negligible [5].

In order to extract the HMW phase, we perform measurements with the voltage only to get the polarizability phase $\varphi_E(V)$ and with the current only to get the Zeeman phase $\varphi_B(I)$, and we then get $\varphi_{EB}(V, I)$:

$$\varphi_{EB}(V, I) = \varphi_{E+B}(V, I) - \varphi_E(V) - \varphi_B(I) \quad (4)$$

The diffraction phase φ_d is very sensitive to the x -positions of the standing wave mirrors M_i , with $\delta\varphi_d/\delta x_i \approx 20$ rad/ μm for M_1, M_3 or 40 rad/ μm for M_2 . This sensitivity induces phase drifts, near 2 rad/hour, due to small displacements δx_i of thermal origin. To minimize the effect of these drifts, we alternate voltage-current configurations over a 20 second-long fringe scan, during which the phase drift is linear and it only mod-

ifies slightly the scan slope. We have used either a 4-field configuration with the following (V, I) values $(0, 0)$, $(V, 0)$, (V, I) , $(0, I)$ or a 6-field configuration including E -reversal, by adding $(-V, 0)$, $(-V, I)$. Fits extract the characteristics of the individual fringe patterns (see fig. 2). If $\varphi(V, I)$ is the fringe phase of the (V, I) configuration, the phases needed to evaluate equation 4 are given by the following differences, $\varphi_E(V) = \varphi(V, 0) - \varphi(0, 0)$, $\varphi_B(I) = \varphi(0, I) - \varphi(0, 0)$ and $\varphi_{E+B}(V, I) = \varphi(V, I) - \varphi(0, 0)$. The statistical uncertainty on $\varphi_{EB}(V, I)$, near 30 mrad for a 20 second-long scan, is reduced near 3 mrad by averaging about 100 scans.

The phase shift thus deduced is still influenced by various stray phase shifts due to geometrical defects of the interaction region [5]. These systematic effects have been studied for a large set of (V, I) data points and an approximate analytical model was developed in order to evaluate their contributions to φ_{EB} . As the stray phase shifts increase rapidly with I , we discuss here only the data collected with $|I| \leq 12$ A, but the experiments carried with larger $|I|$ -values have been useful to understand experimental defects. The dominant part of the stray phase shifts is an even function of I and we separate it from φ_{HMW} which is odd with V and I by combining measurements with opposite I -values in $\varphi_{final} = [\varphi_{EB}(V, I) - \varphi_{EB}(V, -I)]/2$. Similarly as for the Zeeman phase shifts, cancelations between hyperfine sublevels limit the contribution of the Aharonov-Casher effect to very small values in φ_{EB} ; this contribution, always smaller than 3 mrad, was evaluated thanks to our model and subtracted from the data plotted in fig. 3. Our results agree with the expected linear dependence $\varphi_{HMW} \propto VI$, but the slope $\varphi_{final}(V, I)/(VI) = (-1.68 \pm 0.07) \times 10^{-6}$ rad/(V.A) differs by 31% from the expected value, presumably due to a lack of accuracy of our analytical model [5].

The magnetic field direction changes over the interferometer, thus inducing a Berry's phase [2]. The measured Berry's phase is the difference between the two arms and it is expected to be very small because of the magnetic field homogeneity. Moreover, it is canceled by our procedure because it has the same value in $\varphi_{E+B}(V, I)$ and in $\varphi_B(I)$. The more complex Berry's phase involving the electric and magnetic fields discussed in [28] also appears to be negligible [5].

In conclusion, we have performed the first experimental test of the He-McKellar-Wilkens topological phase by atom interferometry: this experiment has taken advantage of the high phase sensitivity of our interferometer and of its arm separation. Our measurement is not limited by the interferometer sensitivity but by systematic effects due to several small experimental defects. The slope of the HMW phase $\varphi_{final}(V, I)$ as a function of the VI product differs from the theoretical value and this difference is probably due to a lack of perfect understanding of the corrections due to field gradients and other experimental defects. These defects are small but they could be further reduced by a better design of the

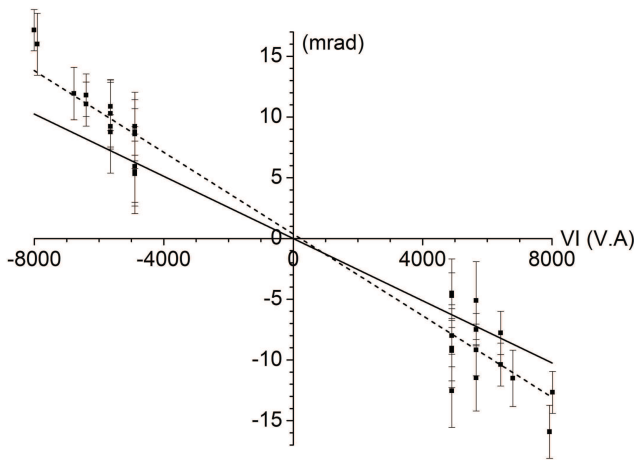


FIG. 3: He-McKellar-Wilkens phase shift as a function of the voltage-current product: the phase $\varphi_{final}(V, I)$ is plotted as a function of the VI product. The data points (squares), represented with their statistical error bars, are in good agreement with a linear behavior $\varphi_{final}(V, I) \propto VI$, as shown by the best fit to the data (dotted line). The fit slope $(-1.68 \pm 0.07)10^{-6}$ rad/V.A is 31% larger than the expected slope of the HMW phase (full line).

interaction region. Moreover, the stray phase shifts due to these defects are enhanced by the fact that the signal is an average over 8 hyperfine-Zeeman sublevels and optical pumping in a single F, m_F sub-level should greatly reduce these systematic effects and improve the accuracy of the

measurements. The HMW phase is expected to independent of the atom velocity v and we can test this property by tuning lithium velocity by changing the supersonic beam carrier gas [5]. This test is feasible and very interesting but we must first reduce the error bar in order to distinguish this behavior from the $1/v$ -dependence of dynamic phases.

This experiment continues the development of new tools in quantum manipulation of atoms. For instance, the HMW effect could be used to build a coherent atom diode based on the non-reciprocal feature of topological phases. While existing atom diodes [29, 30] use optical pumping and do not conserve the coherence of the atom wave, the HMW effect is coherent. In an interferometer as shown in fig. 1, with a HMW phase $\varphi_{HMW} = \pi/2$ for left to right propagation and a diffraction phase $\varphi_d = -\pi/2$, a wave packet would be fully transmitted from entrance A to exit C but a wave packet entering by C would be transmitted to B and not to A. Although very intriguing, such a behavior does not violate any fundamental law and cannot be used to build a Maxwell demon [31].

We thank the laboratory technical staff for their help and A. Cronin for fruitful discussions. The development of our atom interferometer owes much to A. Miffre and to M. Jacquy who also made the first plans of the HMW experiment. We thank CNRS INP, ANR (grants ANR-05-BLAN-0094 and ANR-11-BS04-016-01 HIPATI) and Région Midi-Pyrénées for support.

-
- [1] Y. Aharonov and A. Bohm, *Phys. Rev.* **115**, 485 (1959).
 - [2] Topological phases belong to the group of geometric phases introduced by M.V. Berry (*Proc. R. Soc. Lond. A* **392**, 45-57 (1984)) and reviewed in *Geometric Phases in Physics* by A. Shapere and F. Wilczek (World Scientific ed., Singapore, 1989).
 - [3] Y. Aharonov and A. Casher, *Phys. Rev. Lett.* **53**, 319 (1984).
 - [4] X.-G. He and B.H.J. McKellar, *Phys. Rev. A* **47**, 3424 (1993).
 - [5] See Supplemental Material at [URL will be inserted by publisher] for more details concerning the connection between the AC and HMW phases, the experimental setup, our measurement procedure, the effects of phase shift dispersion, systematic effects and their cancellation in the detection of the HMW phase shift.
 - [6] M. Wilkens, *Phys. Rev. Lett.* **72**, 5 (1994).
 - [7] R.G. Chambers, *Phys. Rev. Lett.* **5**, 3 (1960).
 - [8] A. Tonomura *et al.*, *Phys. Rev. Lett.* **56**, 792 (1986).
 - [9] A. Cimmino *et al.*, *Phys. Rev. Lett.* **63**, 380 (1989).
 - [10] K. Sangster *et al.*, *Phys. Rev. Lett.* **71**, 3641 (1993) and *Phys. Rev. A* **51**, 1776 (1995).
 - [11] A. Görlitz, B. Schuh, and A. Weis, *Phys. Rev. A* **51**, R4305 (1995).
 - [12] K. Zeiske *et al.*, *Appl. Phys. B* **60**, 205 (1995).
 - [13] J.H. Müller *et al.*, *Appl. Phys. B* **60**, 199 (1995).
 - [14] J.P. Dowling, C.P. Williams and J.D. Franson, *Phys. Rev. Lett.* **83**, 2486 (1999).
 - [15] Chia-Chu Chen, *Phys. Rev A* **51**, 2611 (1995).
 - [16] H. Wei, R. Han and X. Wei, *Phys. Rev. Lett.* **75**, 2071 (1995).
 - [17] J. Schmiedmayer *et al.*, in *Atom interferometry* edited by P. R. Berman (Academic Press, San Diego, 1997), p 1-83.
 - [18] Y. Sato and R. Packard, *J. Phys. Conf. Series* **150**, 032093 (2009).
 - [19] N.F. Ramsey, *Phys. Rev.* **78**, 695 (1950).
 - [20] D.W. Keith *et al.*, *Phys. Rev. Lett.* **66**, 2693 (1991).
 - [21] A. Miffre *et al.*, *Eur. Phys. J. D* **33**, 99 (2005).
 - [22] M. Jacquy *et al.*, *Europhys. Lett.* **77**, 20007 (2007).
 - [23] R. Delhuille *et al.*, *Rev. Scient. Instrum.* **73**, 2249 (2002)
 - [24] C.R. Ekstrom *et al.*, *Phys. Rev. A* **51**, 3883 (1995).
 - [25] A. Miffre *et al.*, *Eur. Phys. J. D* **38**, 353 (2006).
 - [26] A.D. Cronin, J. Schmiedmayer, and D.E. Pritchard, *Rev. Mod. Phys.* **81**, 1051 (2009).
 - [27] J. Schmiedmayer *et al.*, *J. Phys. II France* **4**, 2029 (1994).
 - [28] K. Abdullah *et al.*, *Phys. Rev. Lett.* **65**, 2347 (1990).
 - [29] A. Ruschhaupt, J.G. Muga, and M.G. Raizen, *J. Phys. B* **39**, 3833 (2006).
 - [30] J.J. Thorn *et al.*, *Phys. Rev. Lett.* **100**, 240407 (2008).
 - [31] J.C. Maxwell, *Theory of Heat*, 4th edition (Longmans, Green and Co. London, 1875) pp 328-329.